

Predictive Self-Healing Seals for Gas Transmission

Project Number FE0031876

*Michael W. Keller^A, Rami Younis^B, Cem Sarica^B, Mahfujul Khan^A,
Anna Williams^A, Peter Lynch^A, and Ahmed Adeyemi^B*

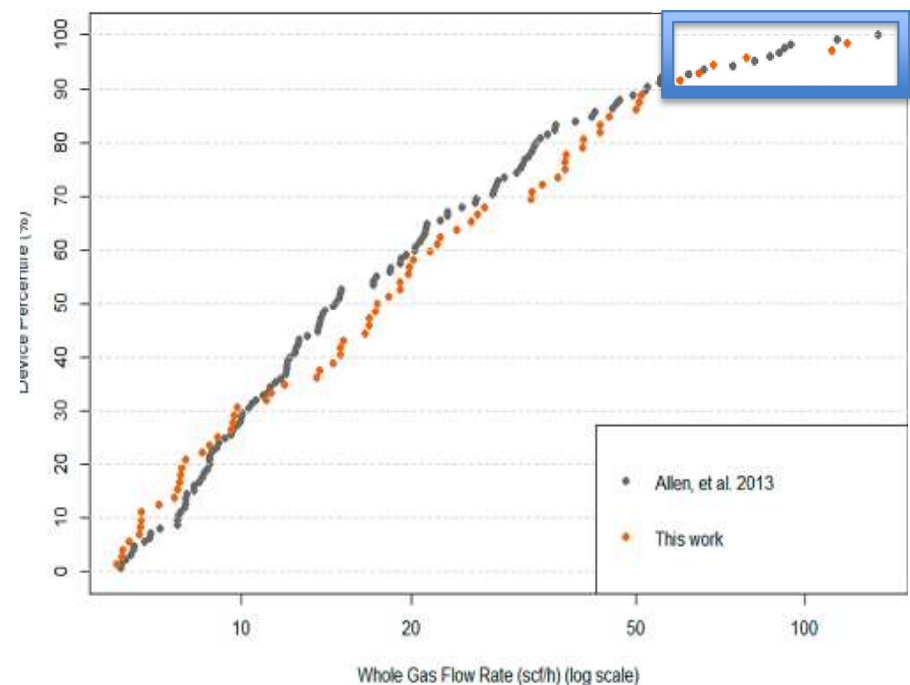
^ADepartment of Mechanical Engineering

^BSchool of Petroleum Engineering

The University of Tulsa

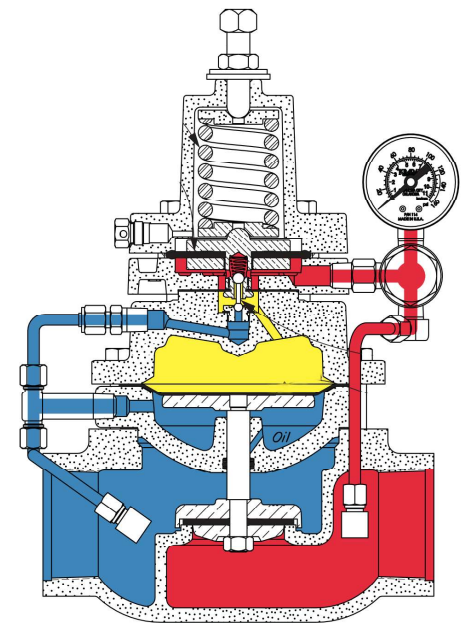
Methane Release from Damaged Systems

- Allen et al.* observed a significant number of anomalous methane releases in pneumatic actuators.
- This project targets 80% reduction of leak rate in those damaged systems.
- Release from damaged systems in the Allen study accounted for 14 million cubic feet of methane/year.
- Milestone goal would reflect a reduction in release by 11 million cubic feet/year for the systems in Allen paper.



Pneumatic Controllers/Actuators

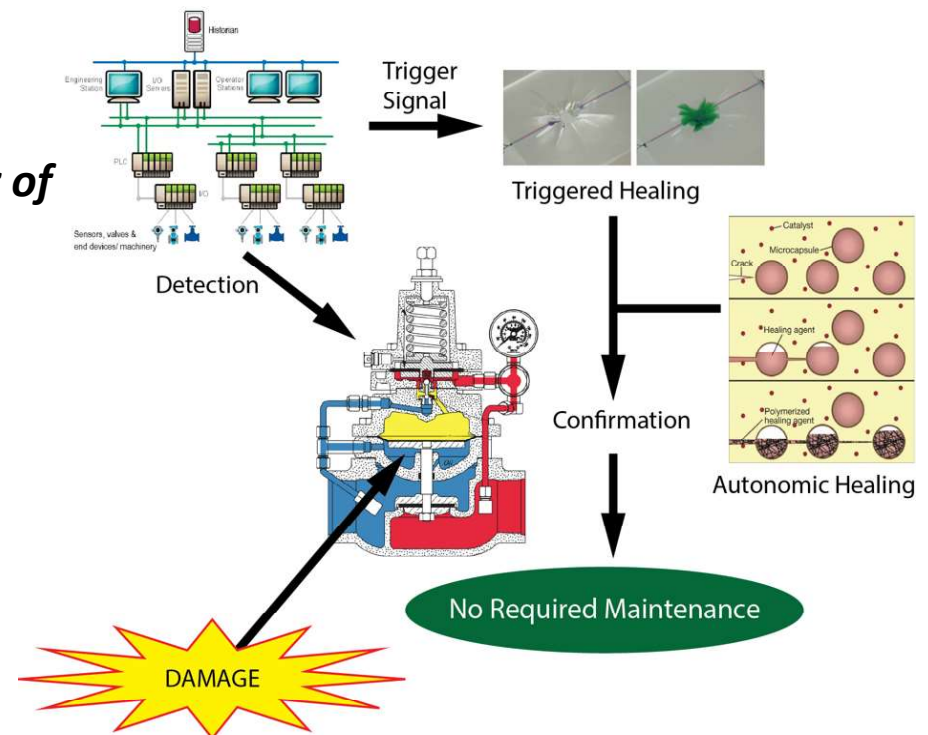
- Various models, but diaphragms are in large number of devices
- Damage can lead to direct venting of natural gas
- Proposed approach is intended to be direct retrofit
- Approach allows for “active” repair
 - Increases healing approach scope
 - Enables repair of large scale damage



Self-Healing Diaphragm

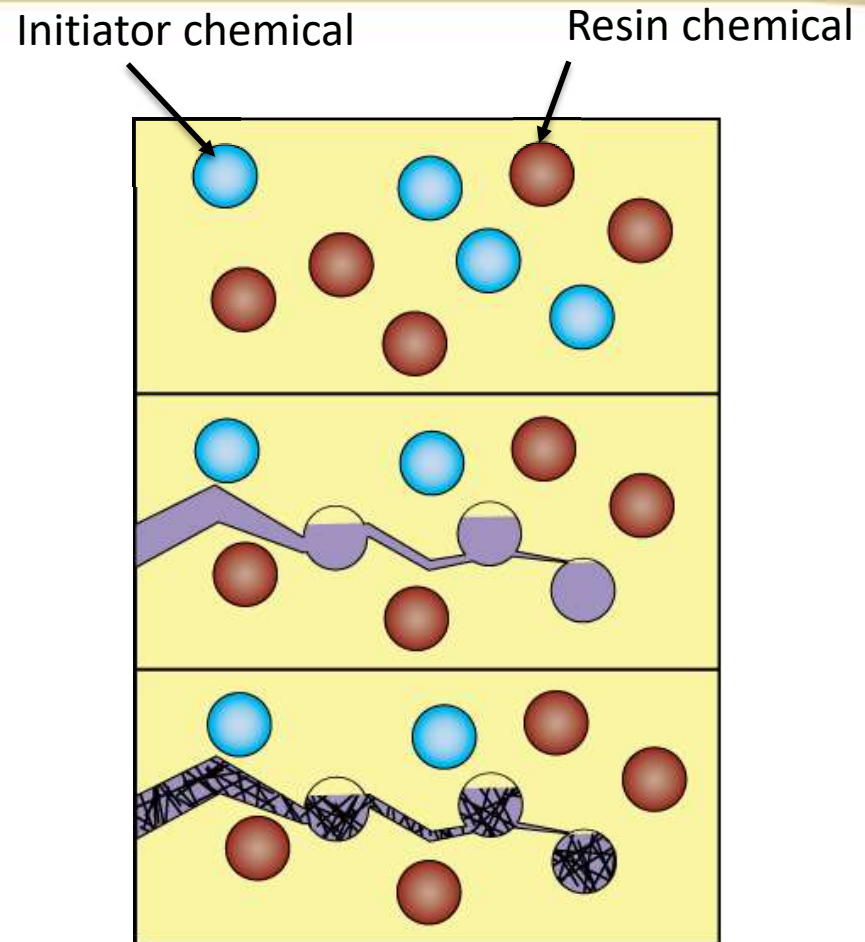
Demonstrate automatic detection and repair of a pneumatic actuator in a pilot scale facility

- Synthesize self-healing system
- Develop detection model
- Build and validate pilot scale test stand



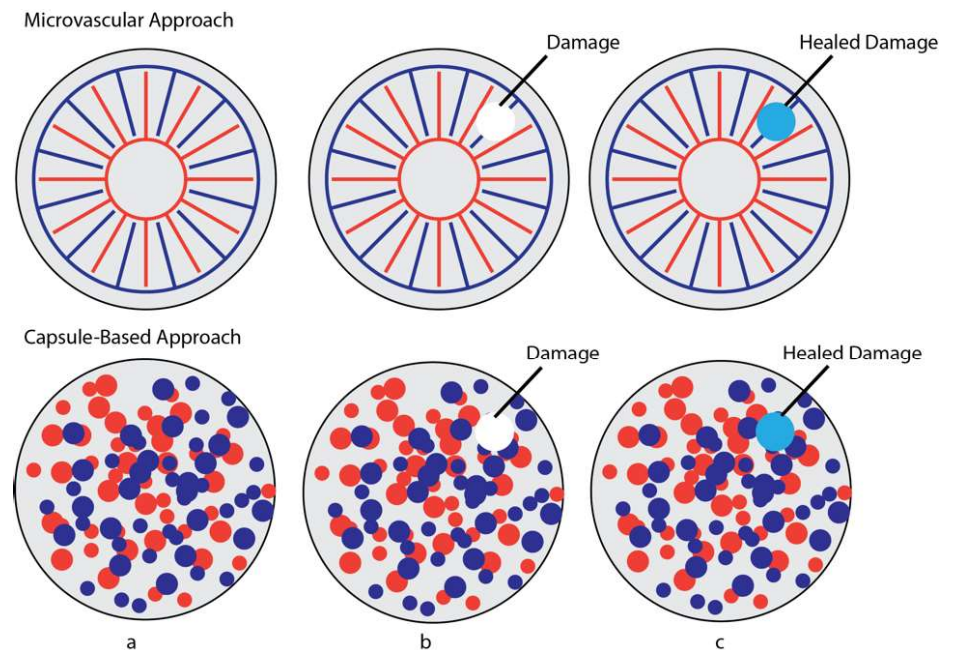
Synthesize Self-Healing Membrane

- Synthesize self-healing membrane material
- Confirm self-repair in laboratory setting
- Integrate system into commercial pneumatic actuator (PA)
- Confirm self-repair in commercial PA.



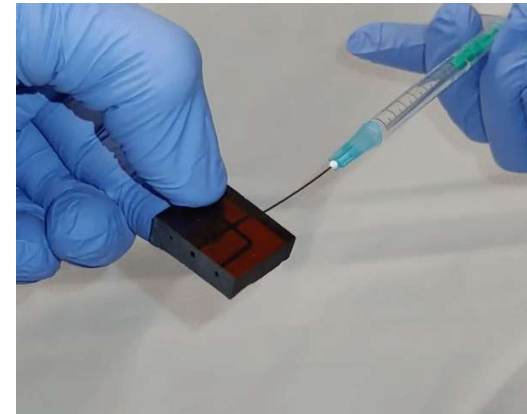
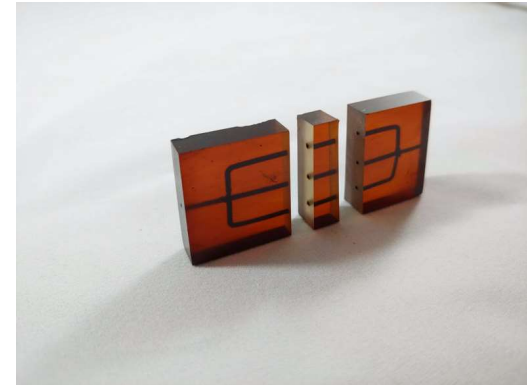
Membrane Processing/Synthesis

- Two approaches
 - Capsule-based repair
 - Microvascular networks
- Initial focus is polyurethane membrane systems
- Siloxane or acrylic-based healing chemistries are initial targets



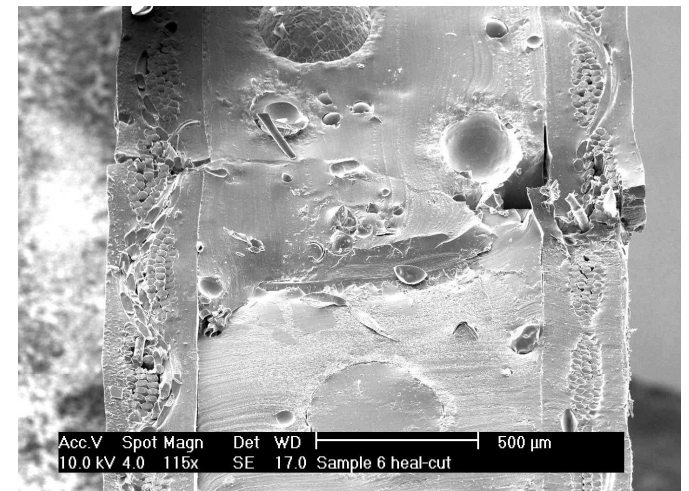
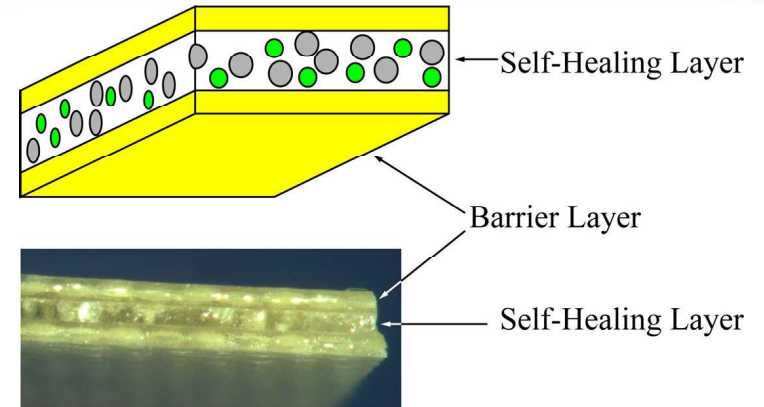
Microvascular Systems

- Based on depolymerization of PLA or other lost-wax approaches
- Channel positive is printed via rapid prototype
- Membrane is cast around positive
- Channels are evacuated to provide circulatory system
- Healing chemistry is circulated in channels
- Monolithic and multilayered systems will be investigated



Capsule-based approaches

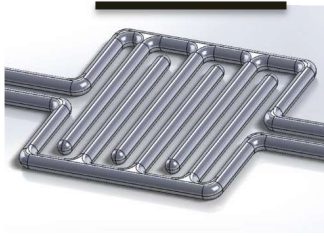
- Based on reactive monomer encapsulation
- Effective for small-scale damage
- Could be combined with microvascular approach for multi-scale repair
- Monolithic and multi-layer systems will be perused



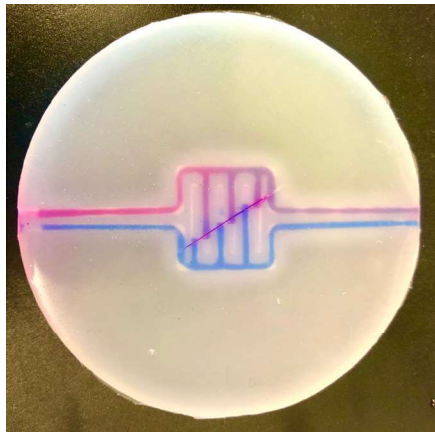
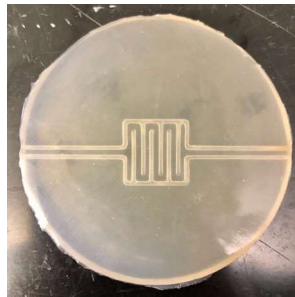
Self-healing Performance

Interdigitated channels

15mm



Hollow channels
PDMS matrix

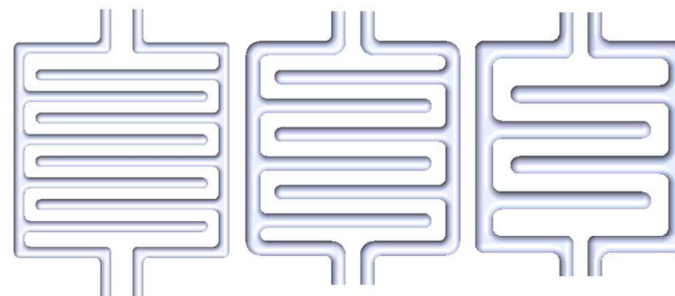


Dyed water in channels

Dimensions
60mm diameter
5mm thick

Original Design

1mm channel diameter
1mm channel spacing

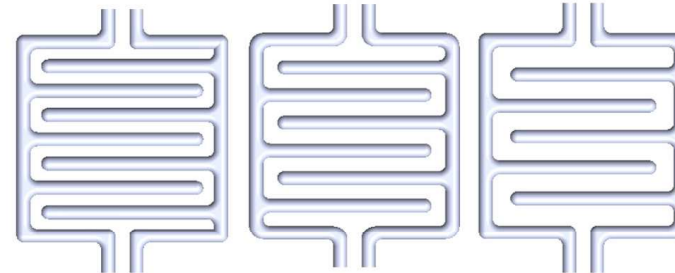


0.75 mm

1.00 mm

1.25 mm

Varying channel
diameter



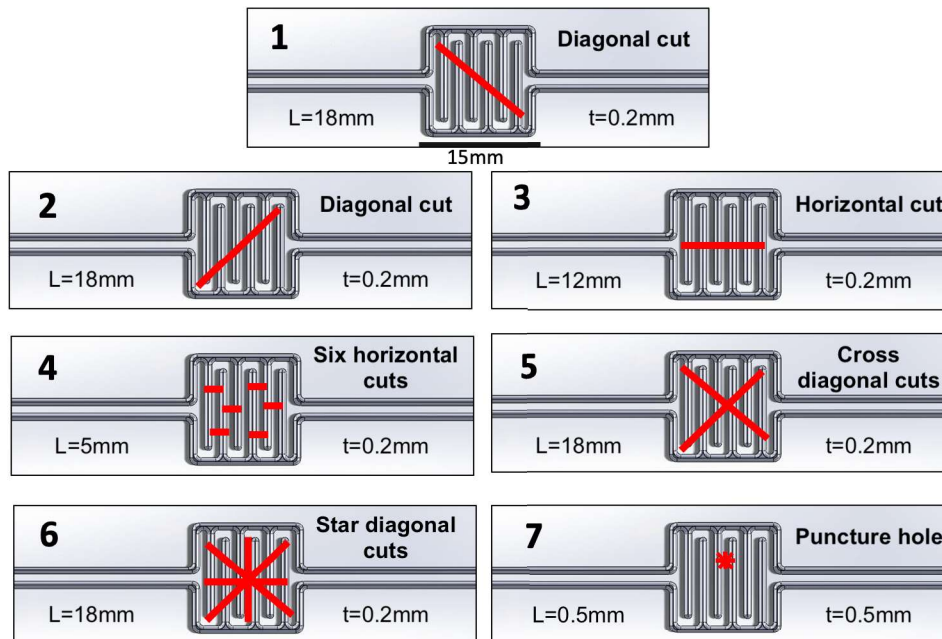
0.75 mm

1.00 mm

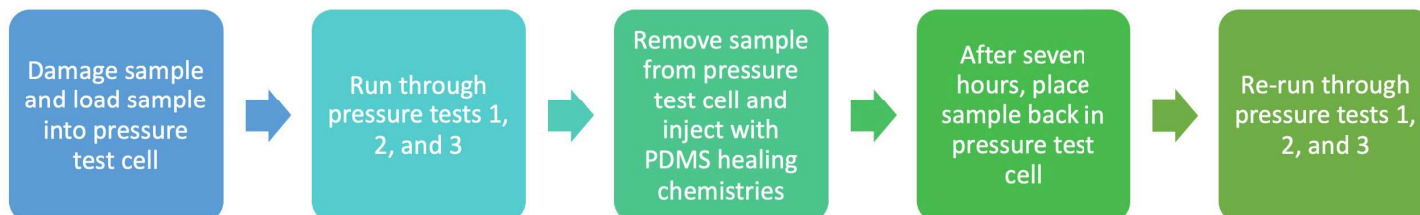
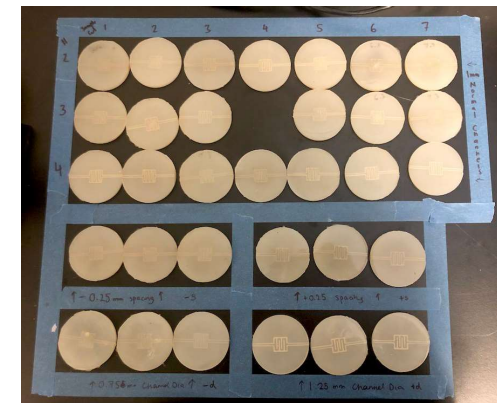
1.25 mm

Varying channel
spacing

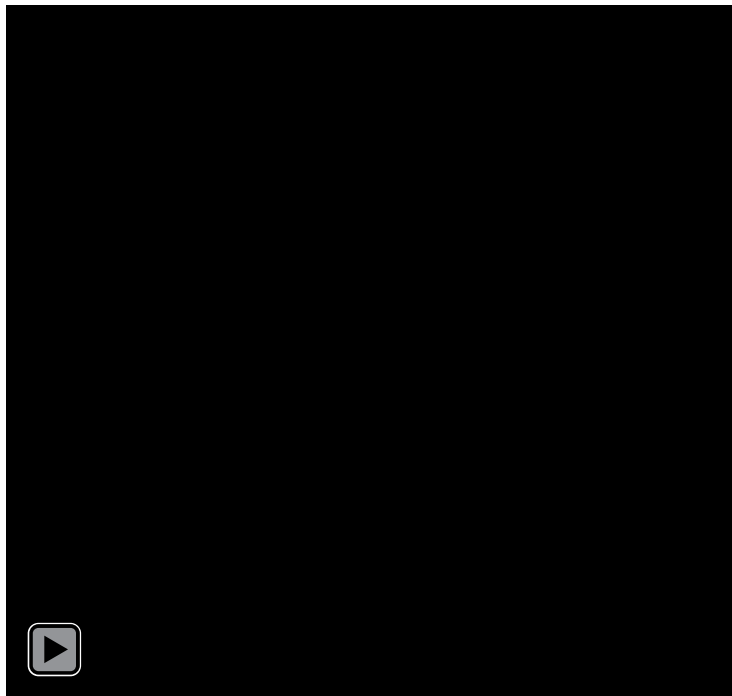
Damage Types and Test Procedure



Type of sample	Number of samples	Damage type(s) applied
Original Design	21	1-7
0.75mm channel diameter	3	1
1.25mm channel diameter	3	1
0.75mm channel spacing	3	1
1.25mm channel spacing	3	1

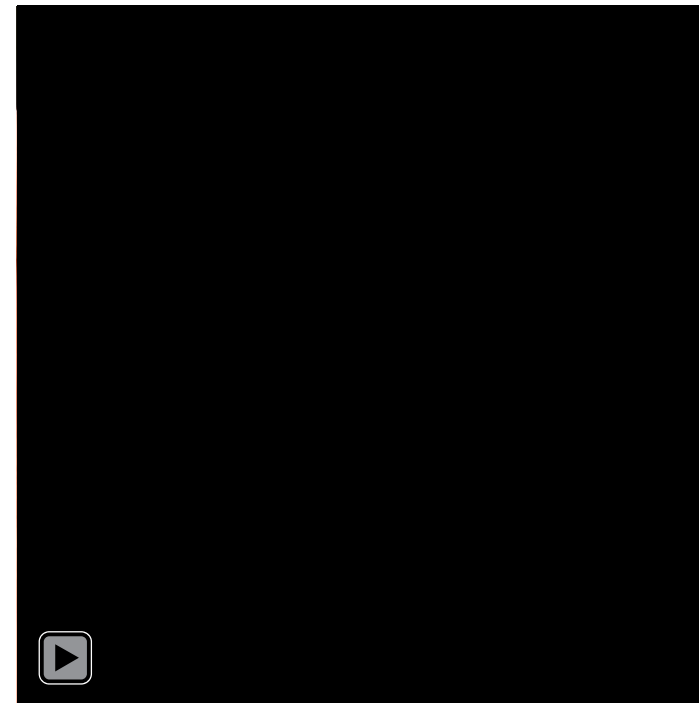



Visual Self-healing Confirmation



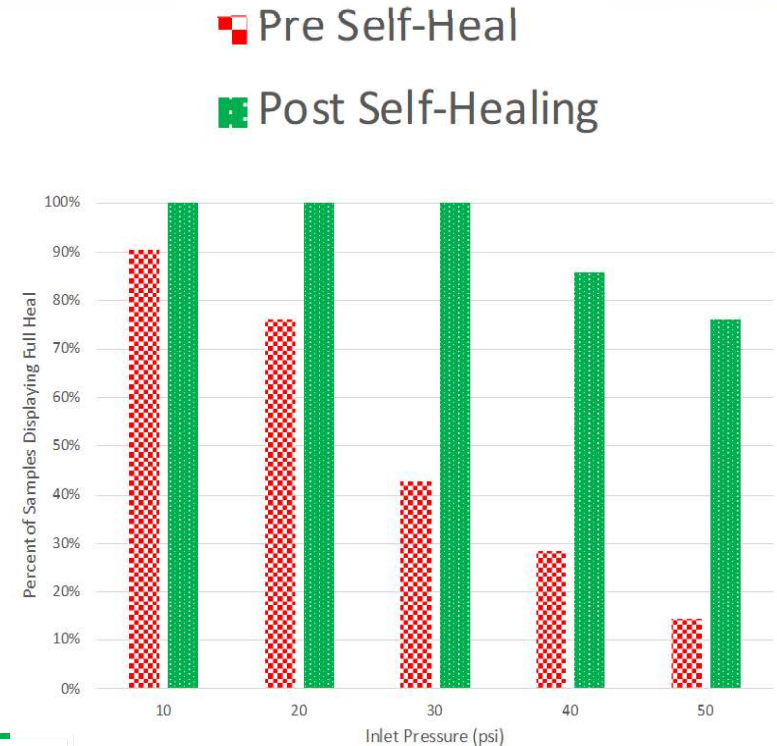
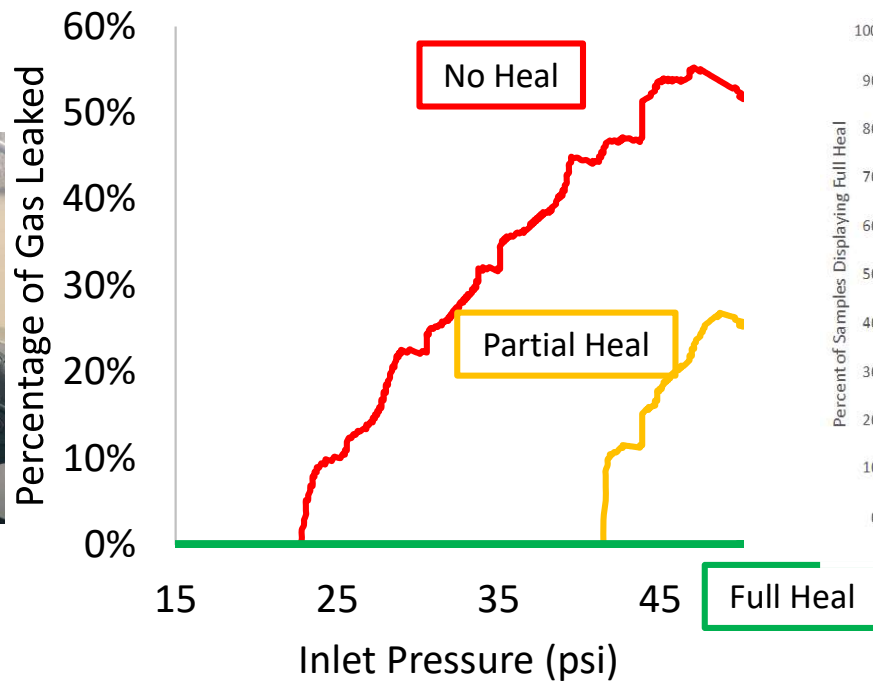
Through thickness damage

Inject
healing
chemistries



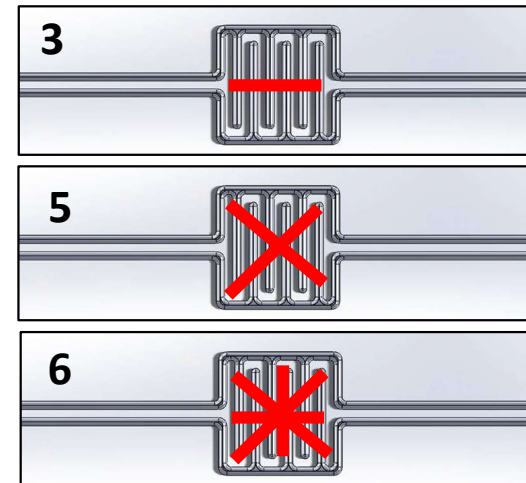
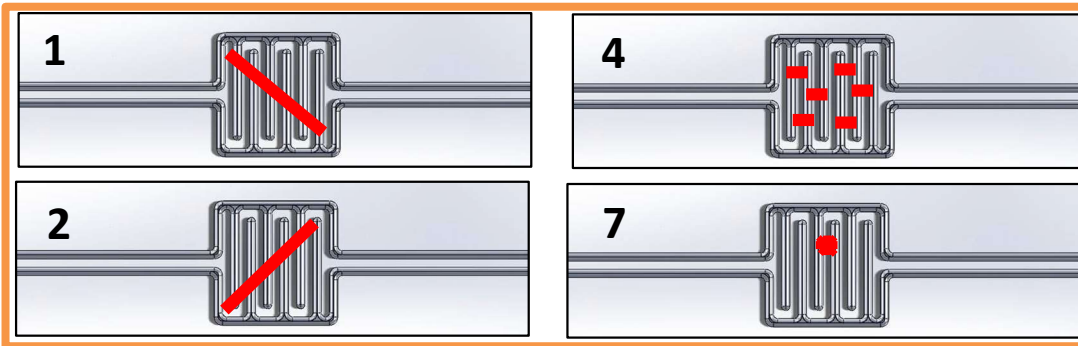
Healing completed

Pressure Test Results



n=21

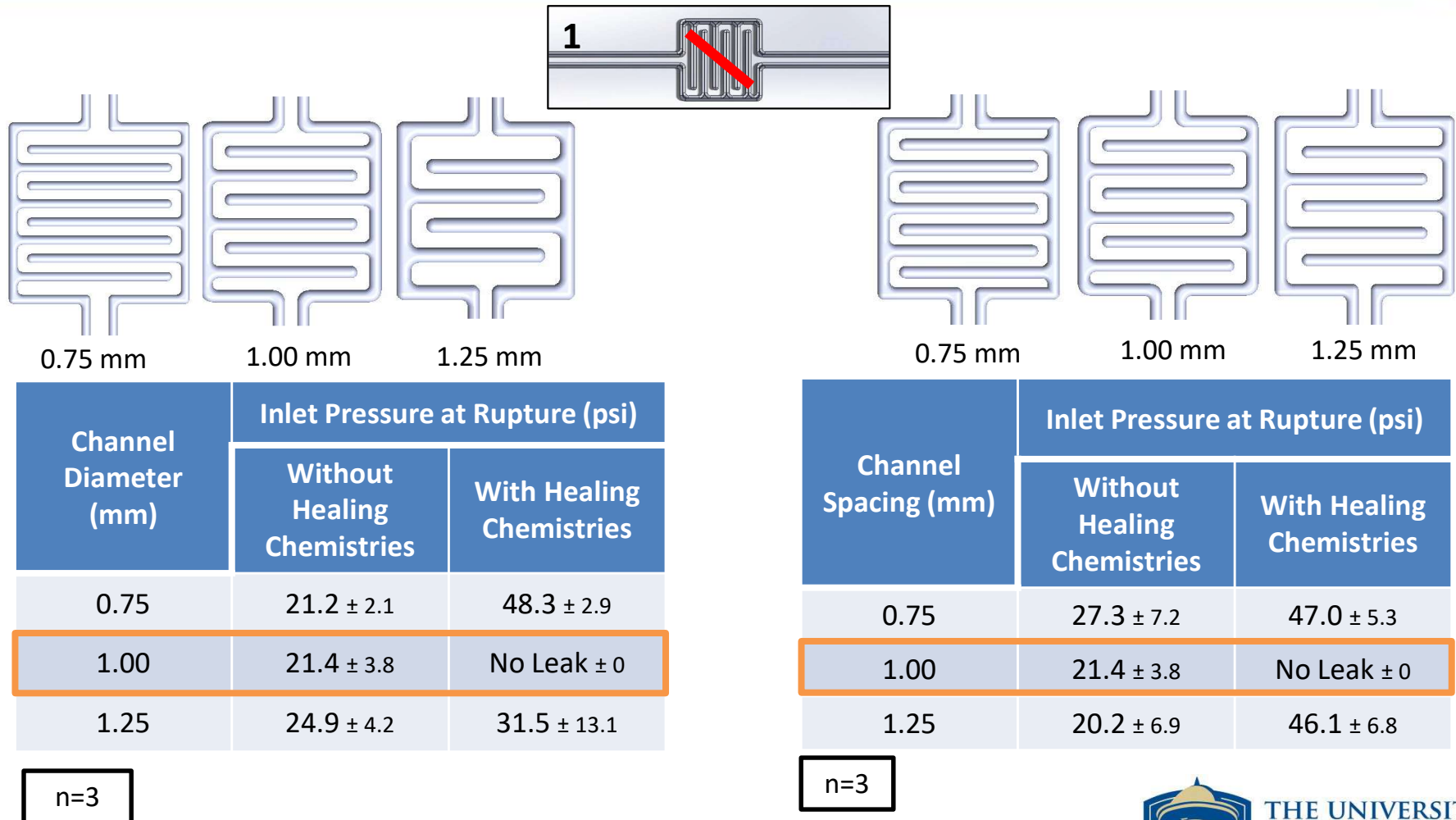
Damage Modes Results



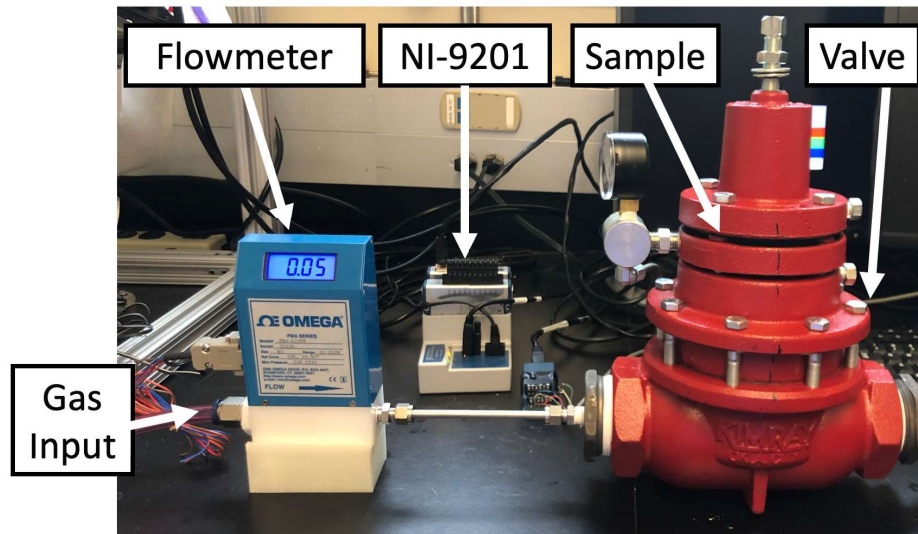
Sample	1	2	3	4	5	6	7
No HC Leak Pressure	21.4 ± 3.8	40.0 ± 4.9	21.6 ± 6.1	42.0 ± 9.0	30.7 ± 17.3	12.3 ± 11.3	No Leak
HC Leak Pressure	No Leak ± 0	No Leak ± 0	49.6 ± 0.7	No Leak ± 0	45.3 ± 8.2	47.6 ± 4.1	No Leak

n=3

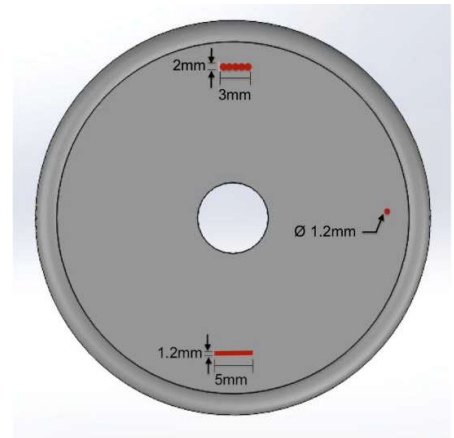
Varying Channel Diameter and Spacing Results



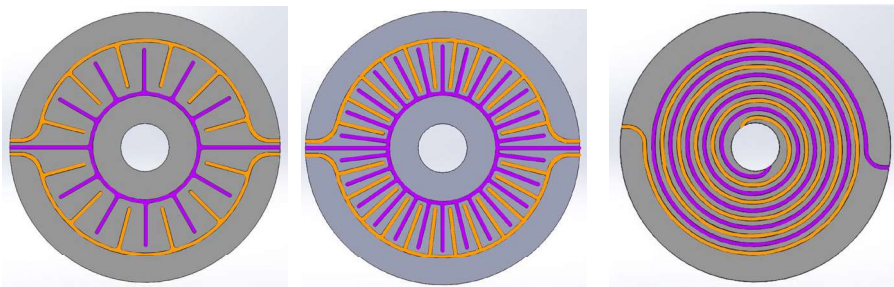
Commercial System



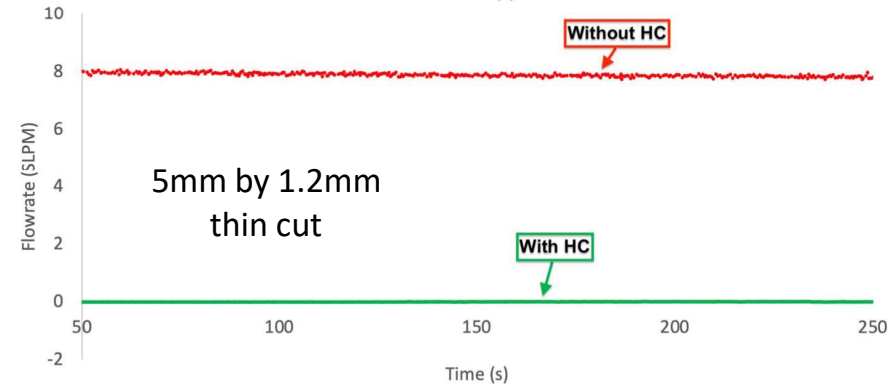
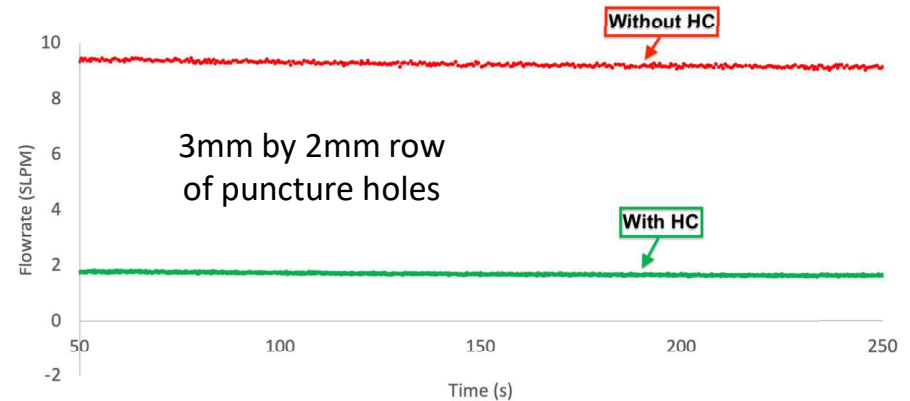
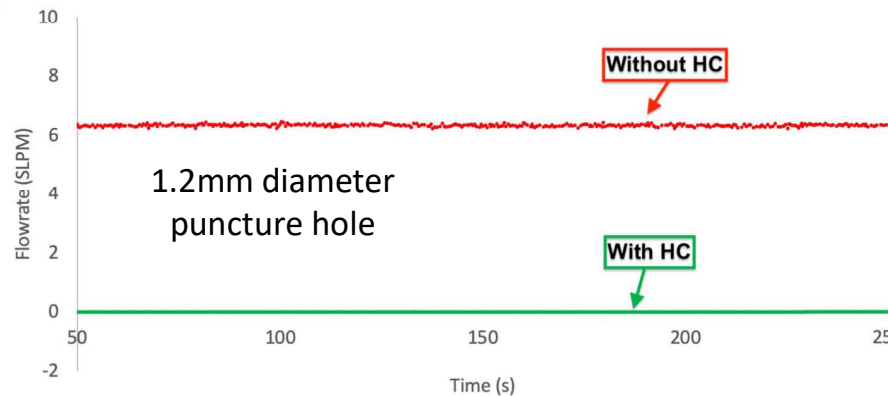
(a) Silicone rubber diaphragm.



(b) Damage types.



Leak Rate Results



81% or greater reduction in leak rate.

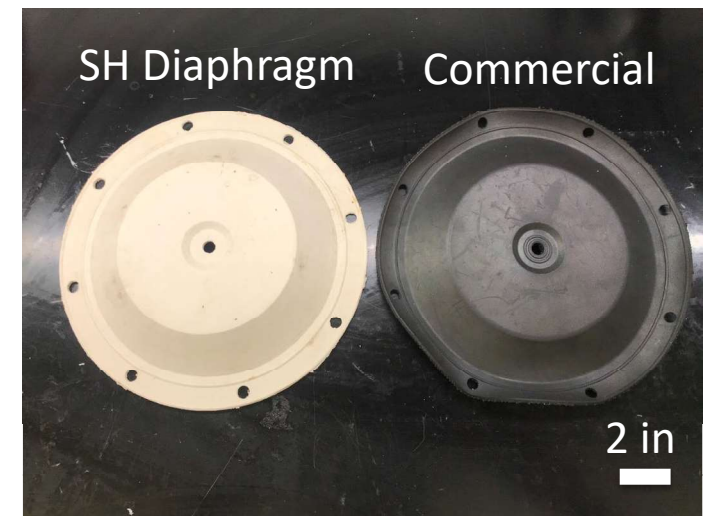
Healing chemistries are more **successful** at healing **thinner cuts** compared to wider damages.

Damage	Before Healing Chemistries	After Healing Chemistries	Leak Rate Reduction
1.2mm by 1.2mm	6.32 ± 0.01	0.05 ± 0.00	100%
3mm by 2mm	9.36 ± 0.06	1.75 ± 0.02	81%
5mm by 1.2mm	7.94 ± 0.00	0.05 ± 0.02	100%

Large Scale Diaphragm Production



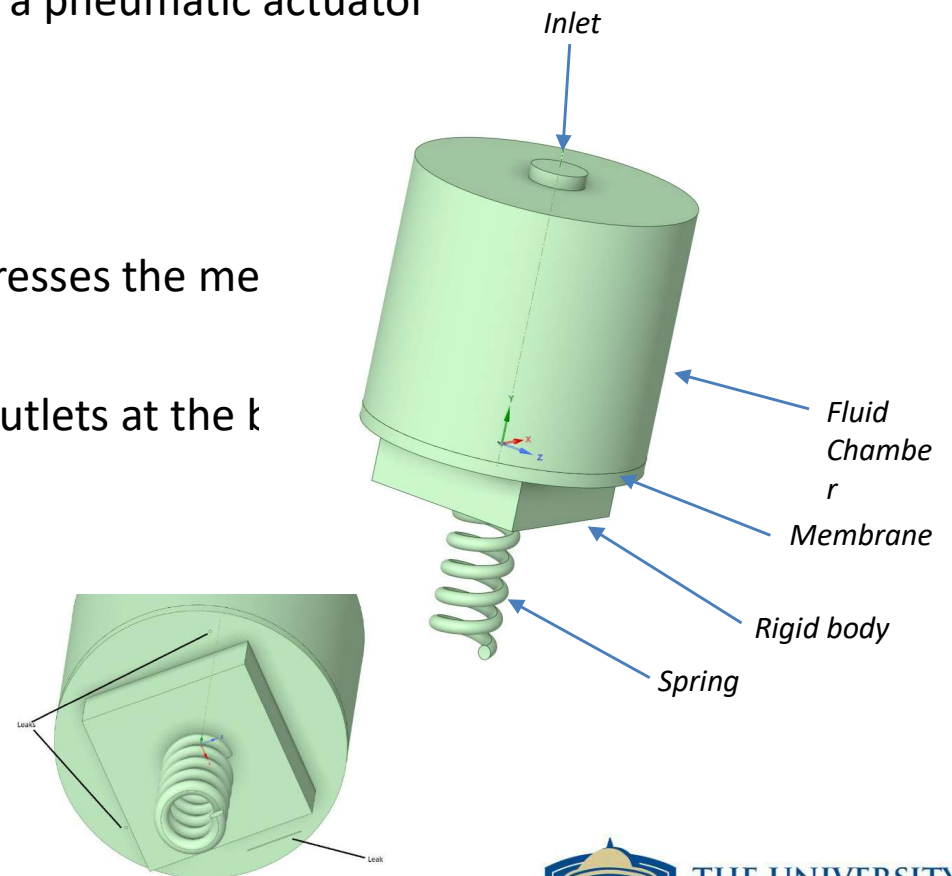
3D Printed Mold



Successful manufacture of a full-scale motor diaphragm with embedded microvascular network.

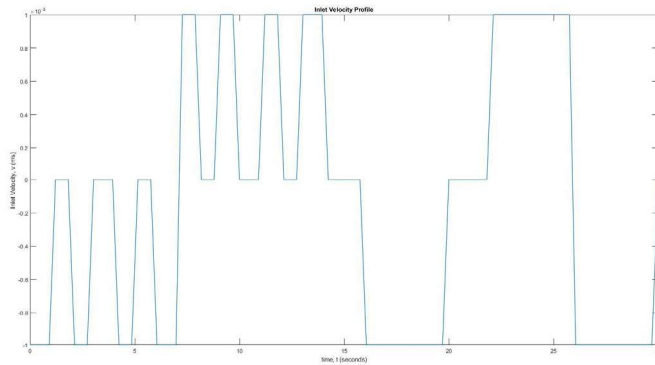
Physics-Based Model Setup

- A three-dimensional high-fidelity numerical model was used to generate a synthetic dataset for the operation of a pneumatic actuator
- Methane is injected at the inlet.
- Pressure buildup in the chamber depresses the me
- Leaks are modelled as tiny pressure outlets at the k

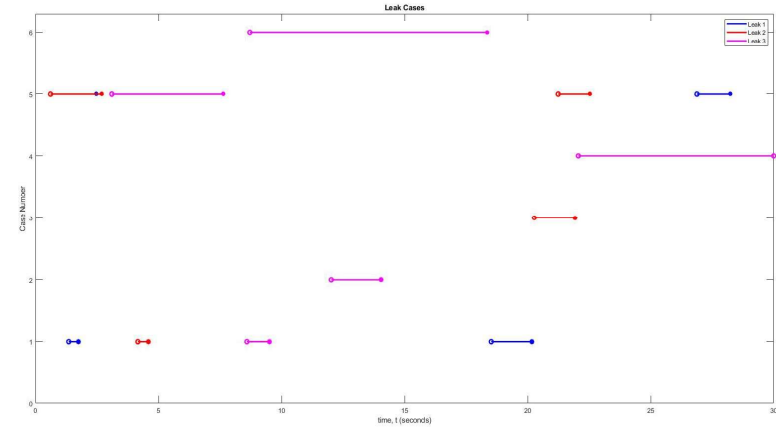


Overview of Dataset

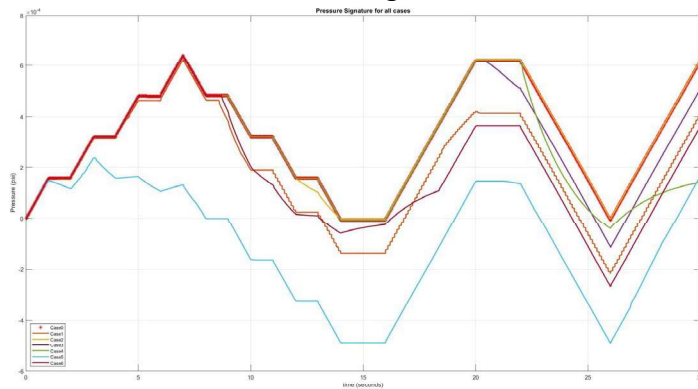
Inlet Rate Schedule



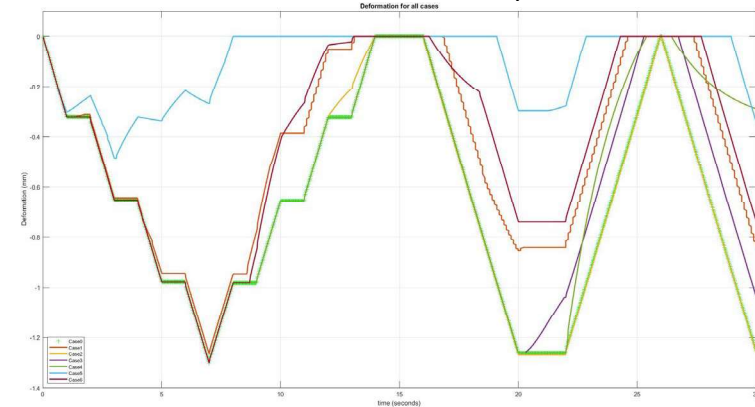
Leak logs



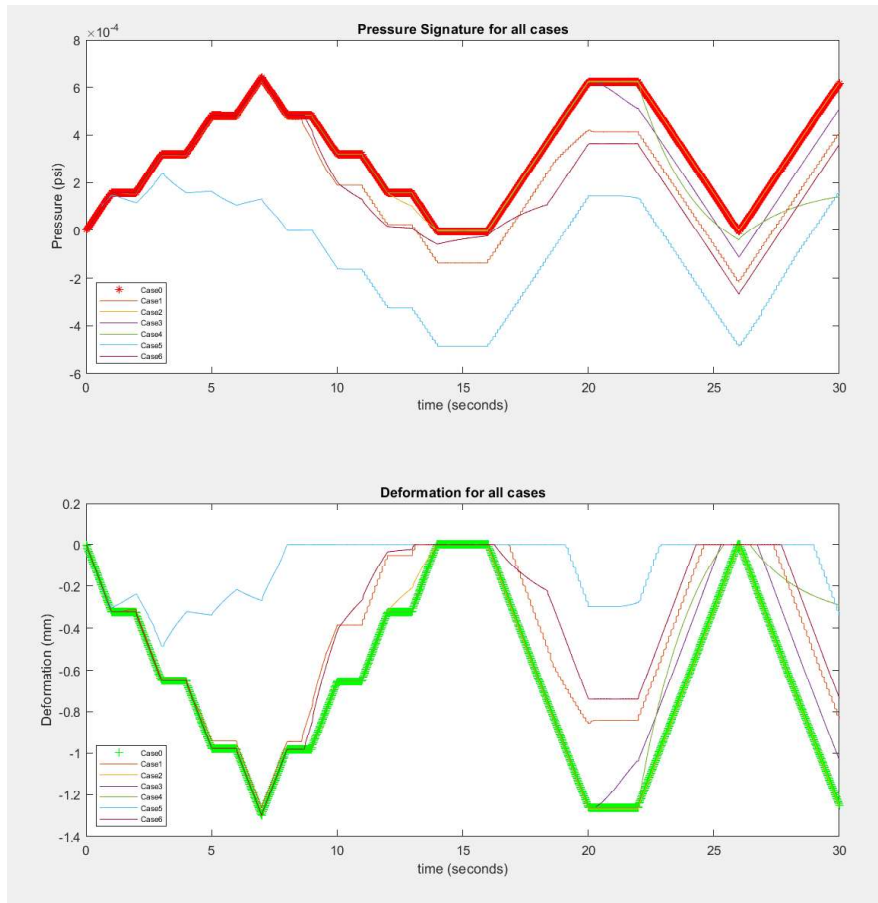
Pressure Signals



Membrane's Vertical Displacement



Review of Dataset

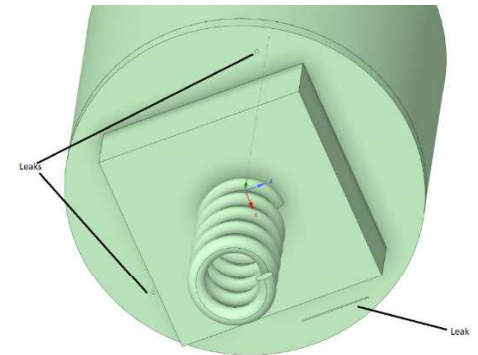


- The complete dataset is comprised of $N=10,500$ entries
- Each data entry is the tuple $d_i = \{t_i, v_i, P_i, y_i, L_i\}$
- L_i is an integer indicator of rupture status

Statistical Methods

- The dataset enables a supervised learning approach
- The response variable Y is a probability of rupture class (0 to 3)
 - 0 - unruptured
 - 1 - circular rupture of diameter 0.1mm on diaphragm edge
 - 2 - circular rupture of 0.1mm near spring-rod attachment, and
 - 3 - tear of length 2mm.
- The features used as predictors at any instant are:

$$x := \left\{ P_i, y_i, \dot{P}_i := \frac{P_{i+1} - P_i}{t_{i+1} - t_i}, \dot{z}_i := \frac{z_{i+1} - z_i}{t_{i+1} - t_i} \right\}.$$



Statistical Methods

- QDA:

$$Pr(Y = k | X = x) = \frac{\pi_k f_k(x)}{\sum_{l=1}^K \pi_l f_l(x)}$$

$$y = \underset{k \in \{0,1,2,3\}}{\operatorname{argmax}} -\frac{1}{2} (x - \mu_k)^T \Sigma_k^{-1} (x - \mu_k) - \frac{1}{2} \log |\Sigma_k| + \log \pi_k$$

- KNN:

$$\hat{Y}(x) = \frac{1}{k} \sum_{x_i \in N_k(x)} y_i$$

- Decision Trees:

$$G = \sum_{k=1}^K p_{mk}(1 - p_{mk})$$

- Bagging:

$$f_{avg}(x) = \frac{1}{B} \sum_{b=1}^B f^b(x)$$

- RF:

$$f_{avg}(x) = \frac{1}{B} \sum_{b=1}^B f^b(x)$$

Results of Simulation

QDA

```
> table(qda.class, Leak.test)
      Leak.test
qda.class 0    1    2    3
0  2716  14    4   22
1    87  52    3    0
2   961  50   64    0
3   711  23    1  542
```

QDA RESULT			
Classes	Total Case	Predicted Case	Percent Accuracy (%)
No Leak	4475	2716	60.69
Leak 1	139	52	37.41
Leak 2	72	64	88.89
Leak 3	564	542	96.10

KNN

```
> table(knn.pred, Leak.test)
      Leak.test
knn.pred 0    1    2    3
0  4424  35    4   40
1    11  99    3    2
2     4    4   65    0
3    36    1    0  522
```

KNN RESULT			
Classes	Total Case	Predicted Case	Percent Accuracy (%)
No Leak	4475	4424	98.86
Leak 1	139	99	71.22
Leak 2	72	65	90.28
Leak 3	564	522	92.55

BAGGING

```
> table(bag.pred, Leak.test)
      Leak.test
bag.pred 0    1    2    3
0  4420  38    3   39
1    17  96    6    2
2     2    4   63    0
3    36    1    0  523
```

BAGGING RESULT			
Classes	Total Case	Predicted Case	Percent Accuracy (%)
No Leak	4475	4420	98.77
Leak 1	139	96	69.06
Leak 2	72	63	87.50
Leak 3	564	523	92.73

Methods	Prediction Accuracy(%)	AUC
QDA	86.91	0.8278
KNN	97.52	0.9439
Decision Tree	96.44	0.9161
Bagging	97.26	0.9412
Random Forest	97.35	0.9434

Ongoing Work

Apply non-dimensional features and augment the data-set with further samples to adequately span the dimensionless parameter space.

Mass Balance

$$(\kappa + Y^*) \frac{\partial P^*}{\partial t^*} + P^* \frac{\partial Y^*}{\partial t^*} = \eta$$

$$Y^* = \frac{y}{y_o}; \quad P^* = \frac{P}{P_o}; \quad t^* = \frac{t}{t_o};$$

$$\kappa = \frac{3H}{2y_o}; \quad \eta = \frac{6t_o ZRT}{\pi P_o y_o L^2 M} (q_{in} - q_{leak})$$

Momentum Balance

$$\alpha \frac{\partial^2 Y^*}{\partial X^{*2}} + P^* = \beta \frac{\partial^2 Y^*}{\partial t^{*2}}$$

$$\alpha = \frac{T y_o}{P_o L x_o^2}; \quad \beta = \frac{\rho y_o}{P_o L t_o^2}$$

Acknowledgments

Research Group:

Mahfujul Khan, PHD

Anna Williams

Peter Lynch

Collaborators:

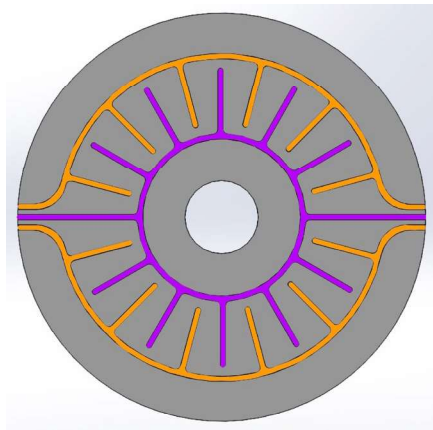
Rami Younis

Ahmed Adeyemi

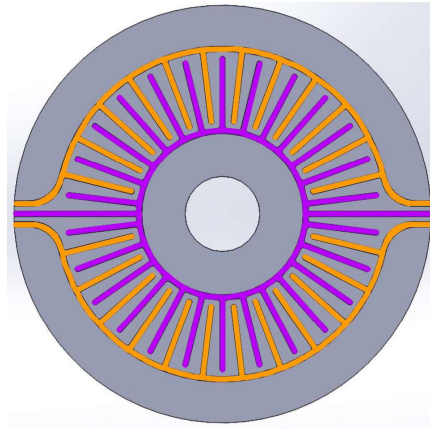
Cem Sarica



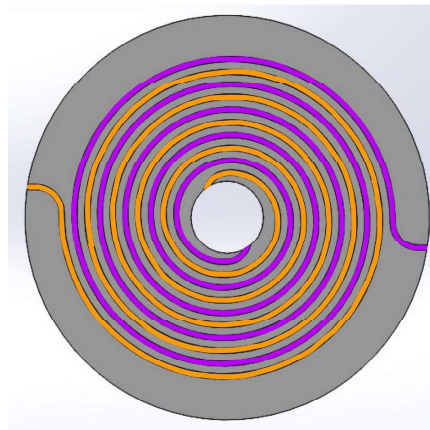
Microvascular Network Geometries



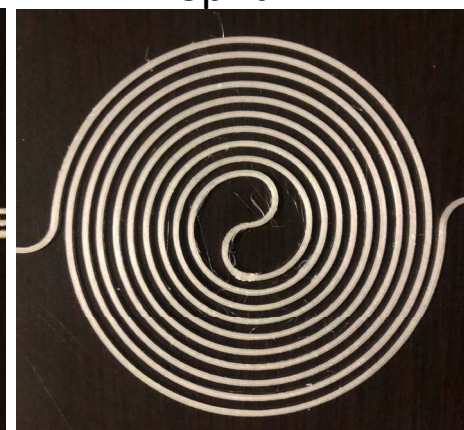
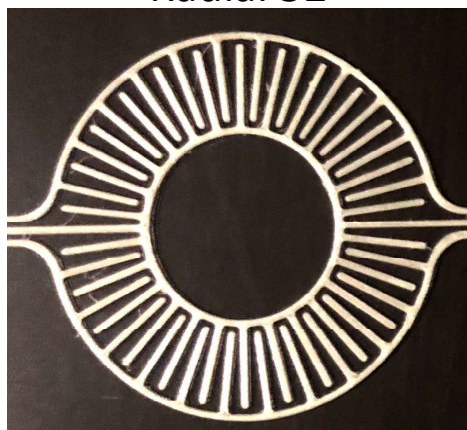
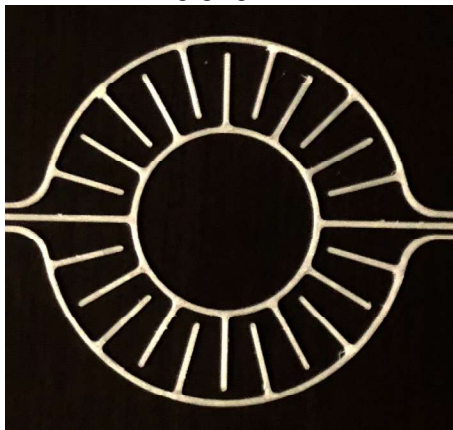
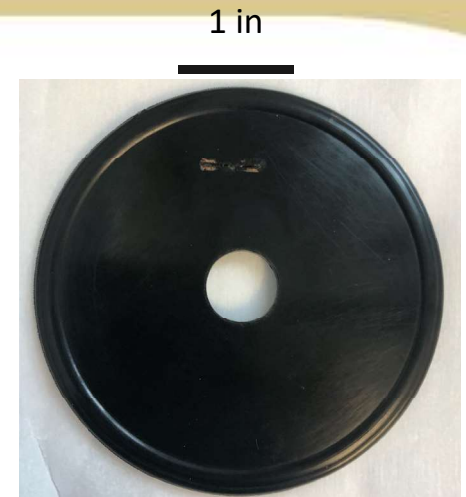
Radial 24



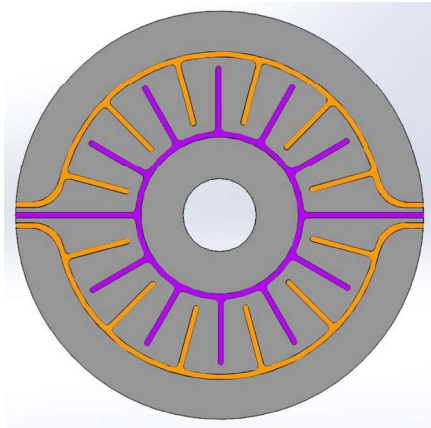
Radial 52



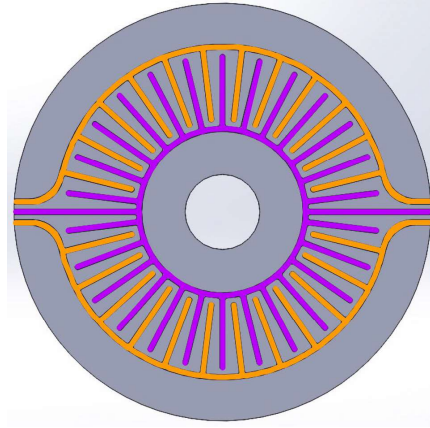
Spiral



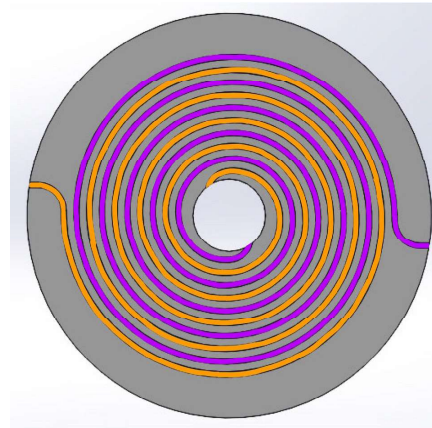
Microvascular Network Geometries



Radial 24

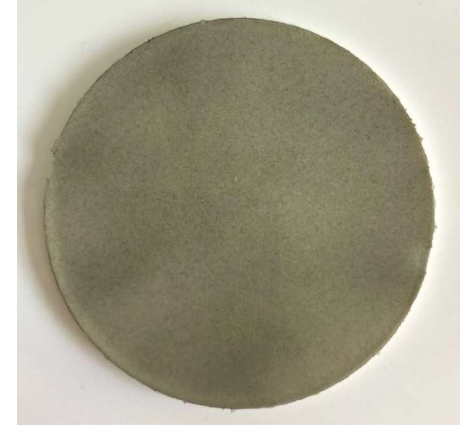


Radial 52



Spiral

1 in



DIC Test Procedure

Load sample
into DIC set-up



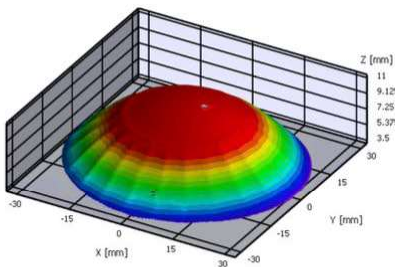
Initiate 5 fps
timed capture
within Vic Snap



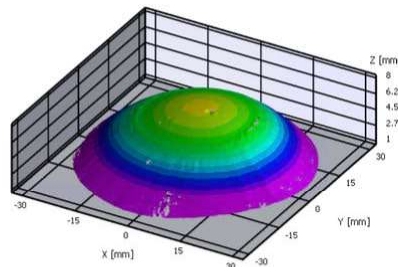
Pressurise
system up to
5psi



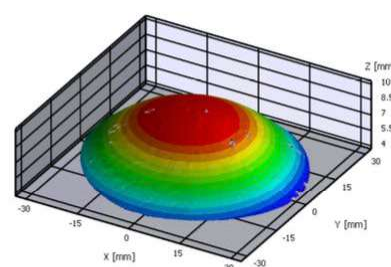
Analyse images
in VIC 3D



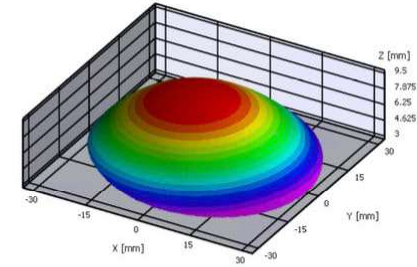
(a) Radial 24.



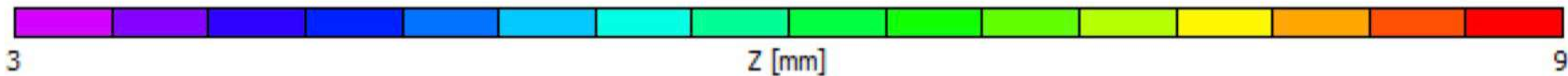
(b) Radial 52.



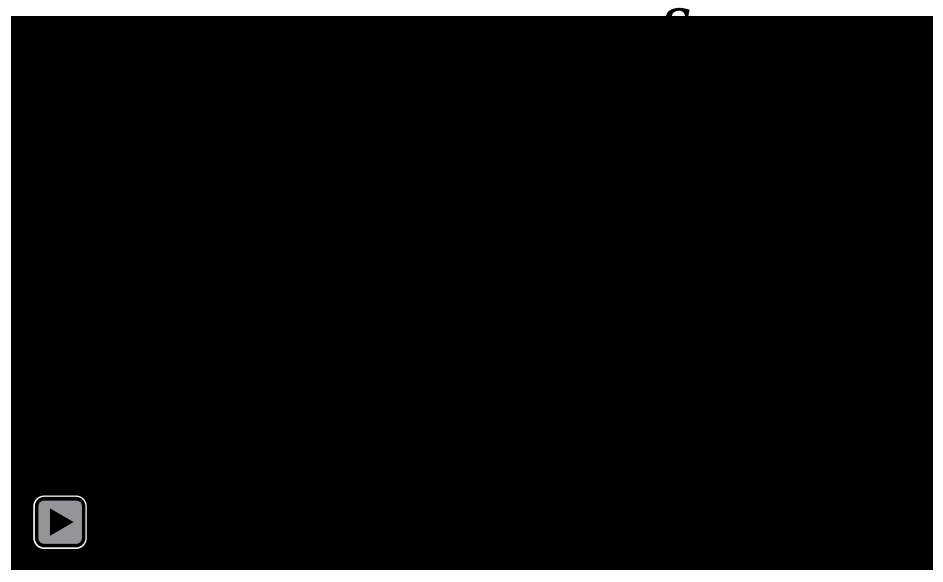
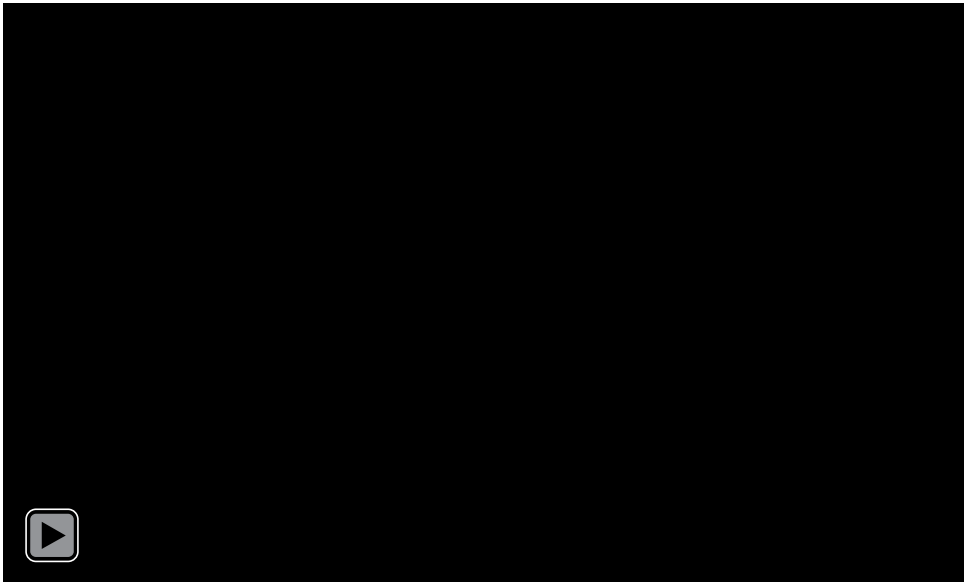
(c) Spiral.



(d) No Channels.

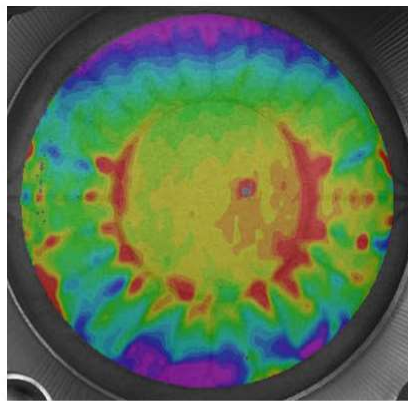


Inflating the Diaphragm

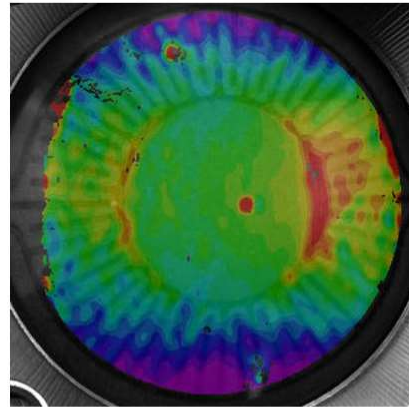


Strain Results for Designs

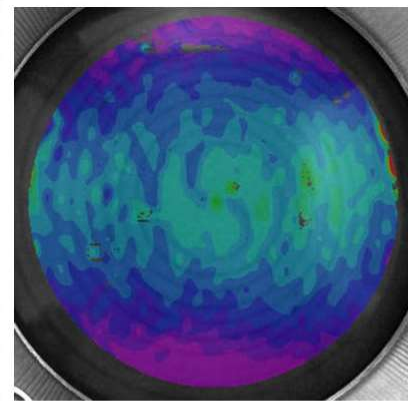
ϵ_{xx}



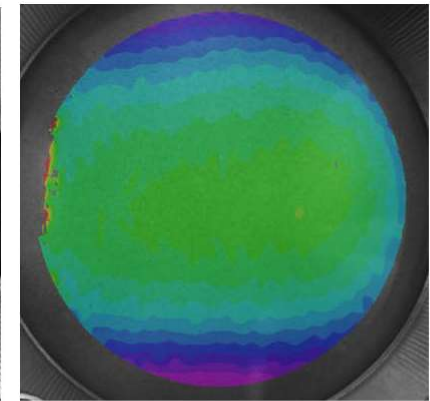
(a) Radial 24.



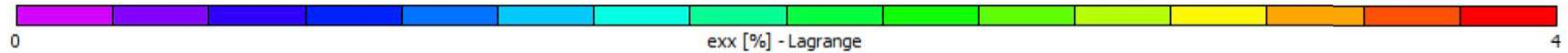
(b) Radial 52.



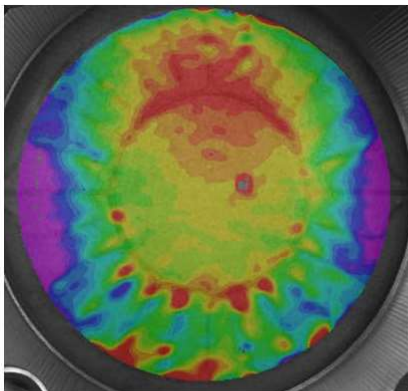
(c) Spiral.



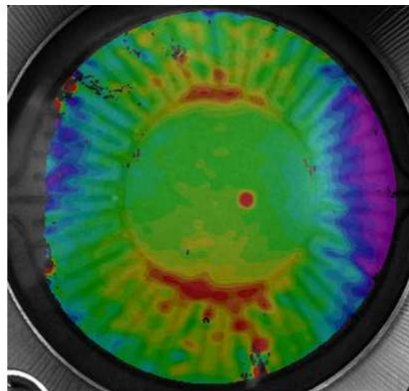
(d) No Channels.



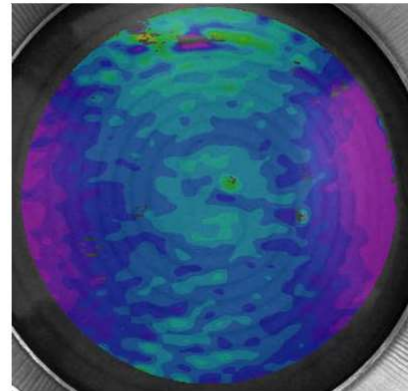
ϵ_{yy}



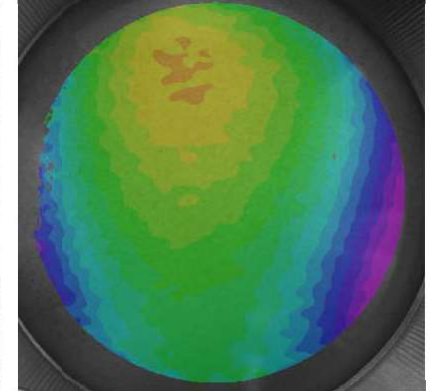
(a) Radial 24.



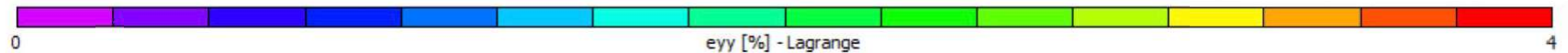
(b) Radial 52.



(c) Spiral.

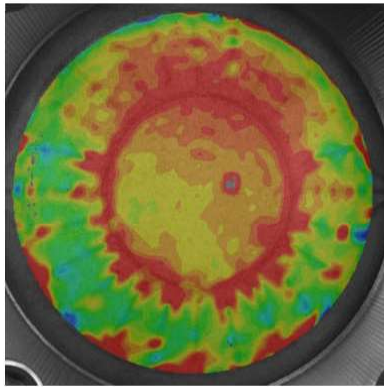


(d) No Channels.

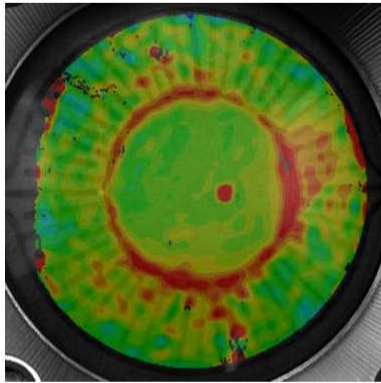


Strain Results for Designs

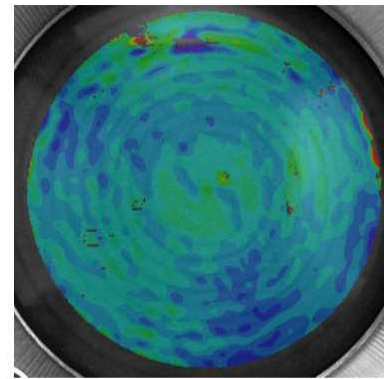
ϵ_1



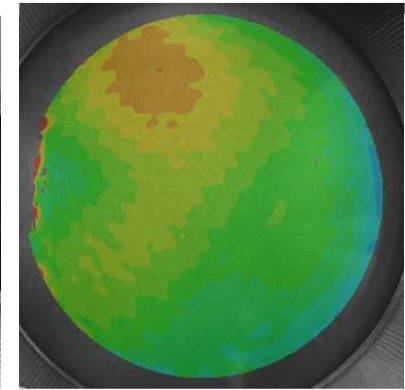
(a) Radial 24.



(b) Radial 52.



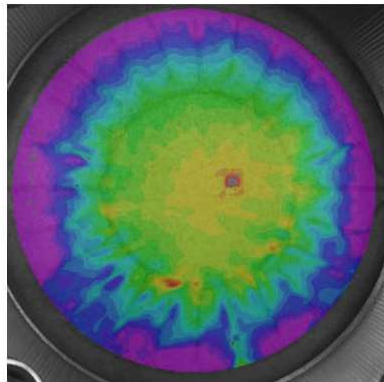
(c) Spiral.



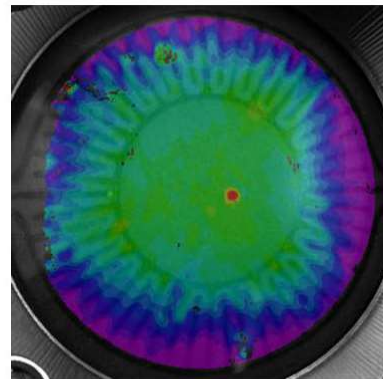
(d) No Channels.



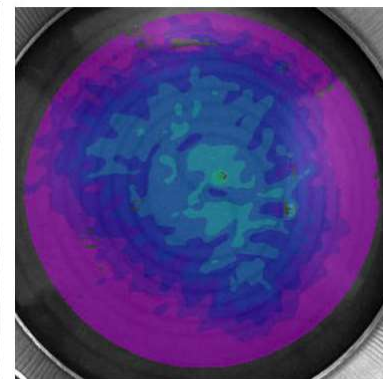
ϵ_2



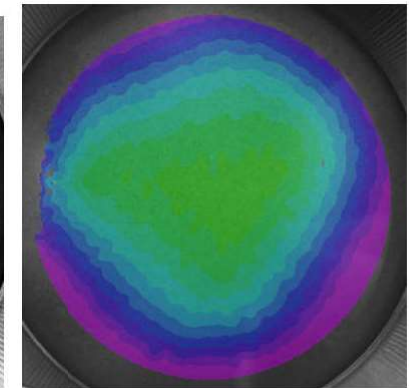
(a) Radial 24.



(b) Radial 52.



(c) Spiral.



(d) No Channels.



Comparison of Maximum Strains

Sample	ϵ_{xx}	ϵ_{yy}	ϵ_{xy}
Radial 24	4.36	4.50	1.46
Radial 52	4.16	3.82	1.11
Spiral	1.93	2.06	0.94
No Channels	2.45	3.26	1.20

Radial 24 had the **highest** strains across all directions

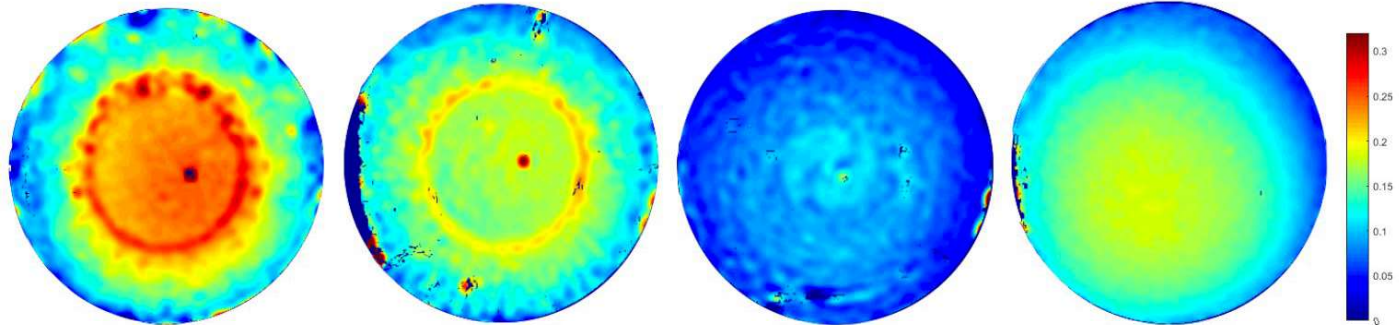
Spiral had the **lowest** strains across all directions

Sample	ϵ_1	ϵ_2
Radial 24	4.88	3.18
Radial 52	4.48	2.48
Spiral	2.39	1.41
No Channels	3.42	2.36

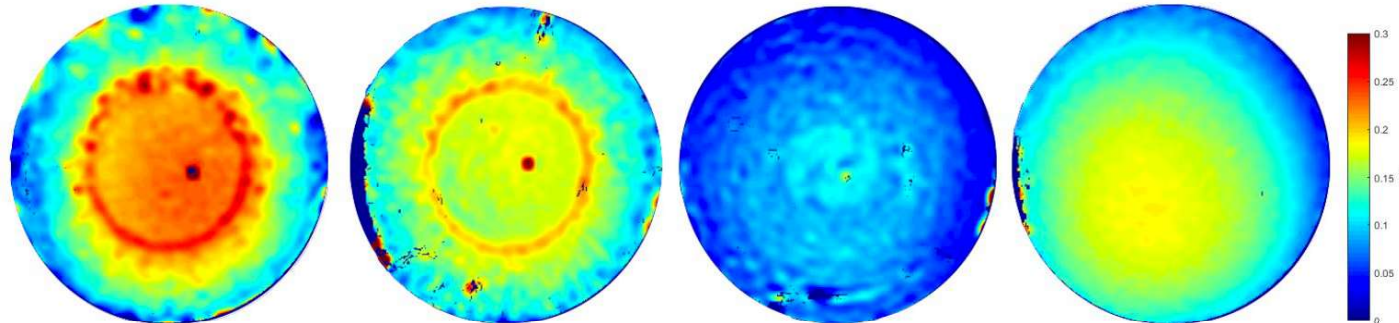
All strain values across all samples are **low** compared to the Elongation at Break (1000%) property of the material

Integration of microchannels into diaphragm materials **would not** significantly interfere with the **integrity** of the material.

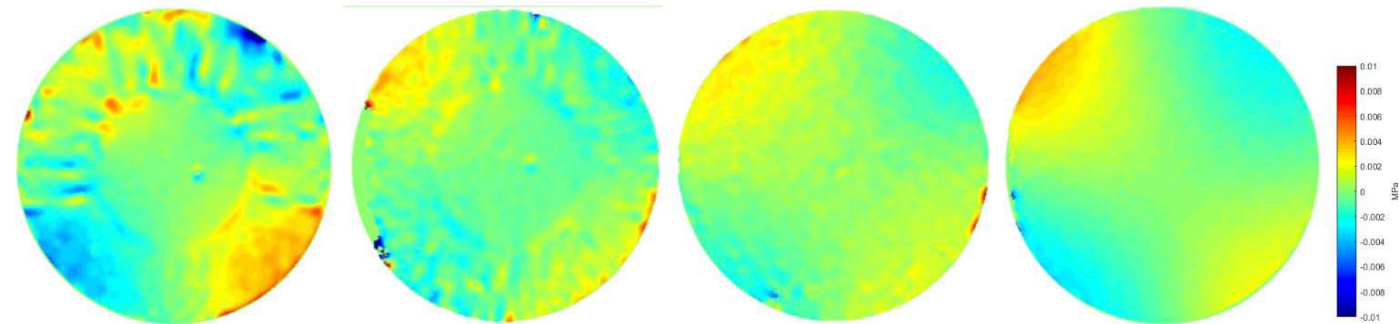
σ_{xx}



σ_{yy}



σ_{xy}



(a) Radial 24.

(b) Radial 52.

(c) Spiral.

(d) No Channels.

$E = 0.42\text{MPa}$
 $\nu = 0.48$
Hooke's Law

Comparison of Maximum Stresses

Sample	σ_{xx}	σ_{yy}	σ_{xy}
Radial 24	0.3733	0.3748	0.0126
Radial 52	0.3126	0.3145	0.0136
Spiral	0.2463	0.2549	0.0115
No Channels	0.2829	0.2688	0.0046

All stress values across all samples are **far below** the material's tensile strength of 3.275 MPa.

Radial 24 had the **highest** stresses across all directions

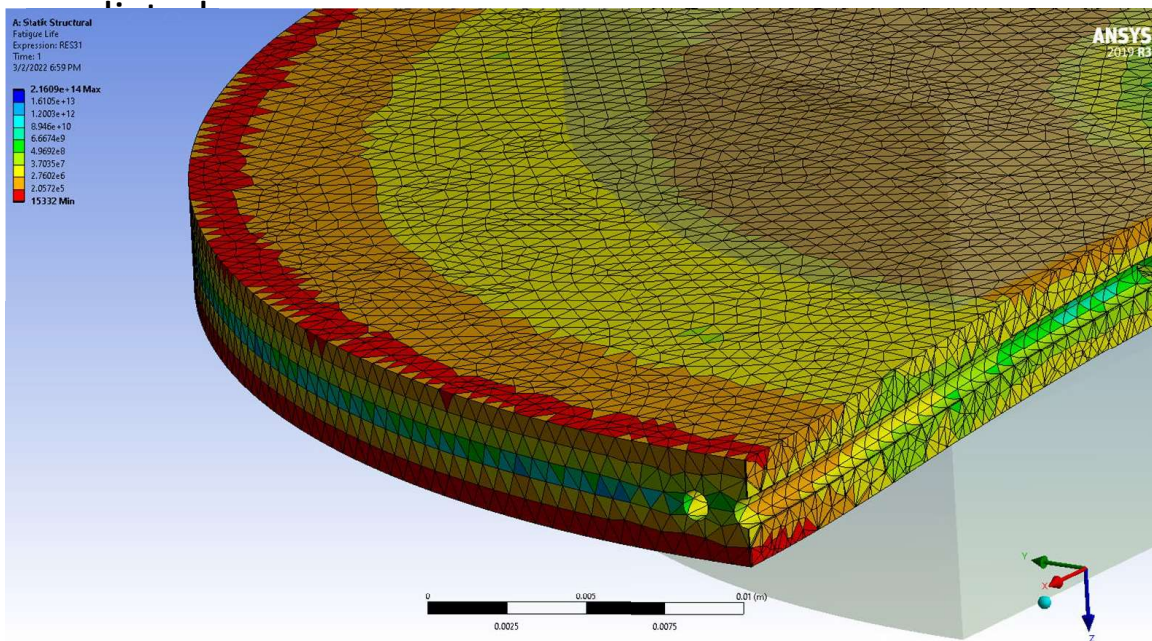
Spiral had the **lowest** stresses across all directions

Remain satisfied that the integration of microchannels into diaphragm materials **would not** significantly interfere with the **integrity** of the material.

Comparison with FEA Simulations



Both experimental and simulation expect stresses around the channels lower than the yield strength of the material, hence no failure at central channels is



Neo Hookean Elasticity Thomas fatigue model predicts failure at edge clamped zone – again agreeing with the life of the material not being compromised by the addition of channels

Simulation by Dr. Khan, University of Tulsa

Appendix

- These slides will not be discussed during the presentation, **but are mandatory.**

Benefit to the Program

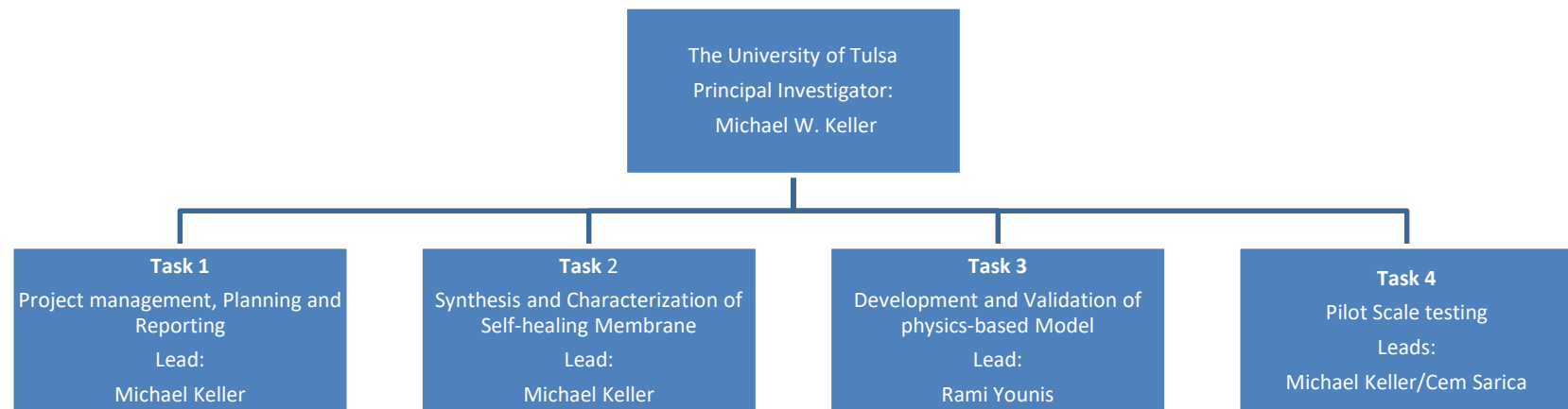
- Reduction of methane release by at least 80%.
- Insert project benefits statement.
 - See Presentation Guidelines for an example.

Project Overview

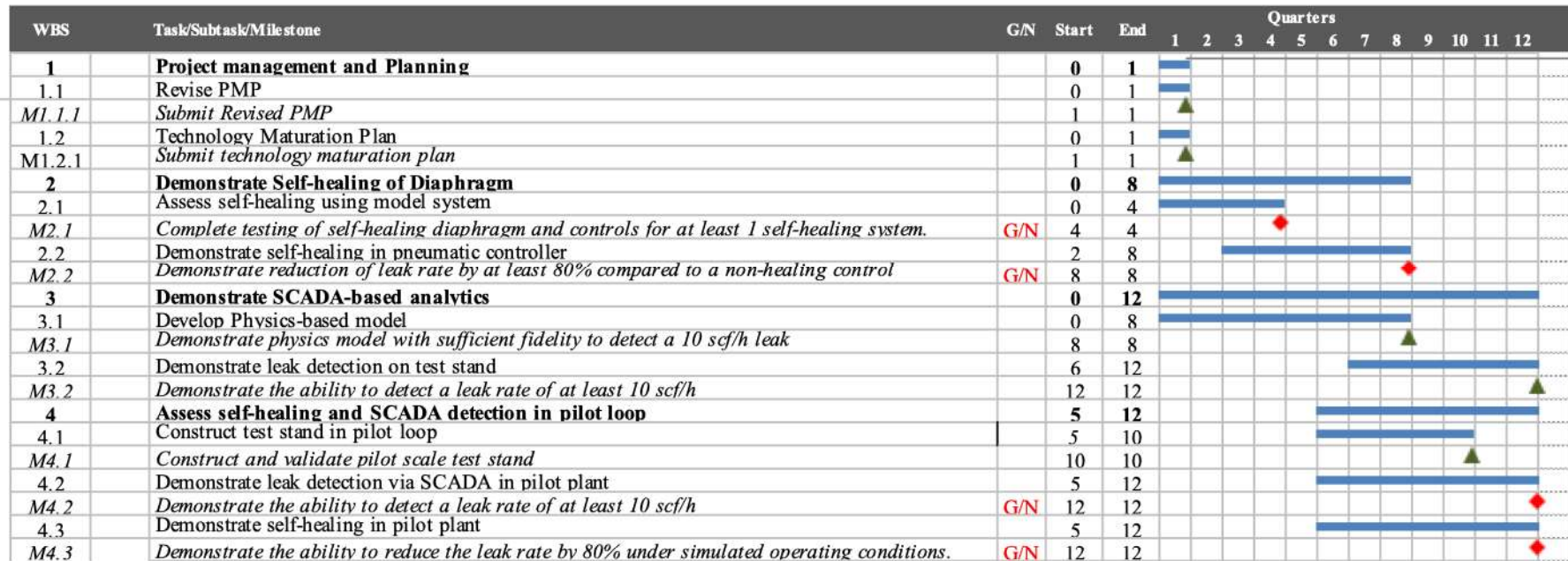
Goals and Objectives

- Demonstrate the ability to automatically repair pneumatic controllers from a wide range of damage.
- Develop appropriate SCADA-based real-time monitoring tools to identify a damaged pneumatic controller
- Develop appropriate SCADA-based tools to determine if self-repair was effective.
- Provide technoeconomic analysis of the proposed system.
- Demonstrate the system in a pilot scale flow loop.

Project Organizational Chart



Gantt Chart



Bibliography

- List peer reviewed publications generated from the project per the format of the examples below.
- None to report